Large-scale Inverse Modeling of Hydraulic Tomography by Physics Informed Neural Network

Presenter: Quan Guo

Advisor: Prof. Jian Luo

Civil and Environmental Engineering

Georgia Institute of Technology

December 2022

AGU FALL MEETING

SCIENCE LEADS THE FUTURE

Groundwater Pumping Test

Pumping test is widely used to investigate porous media property and simulate groundwater (GW) flow.

Porous media

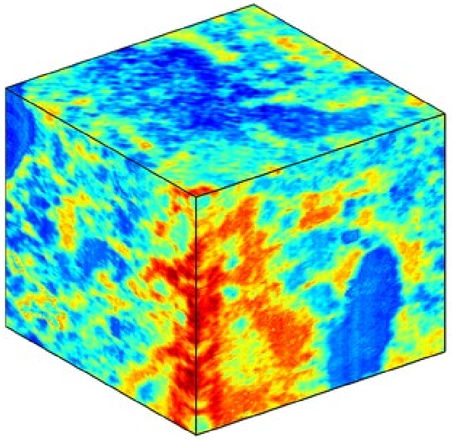

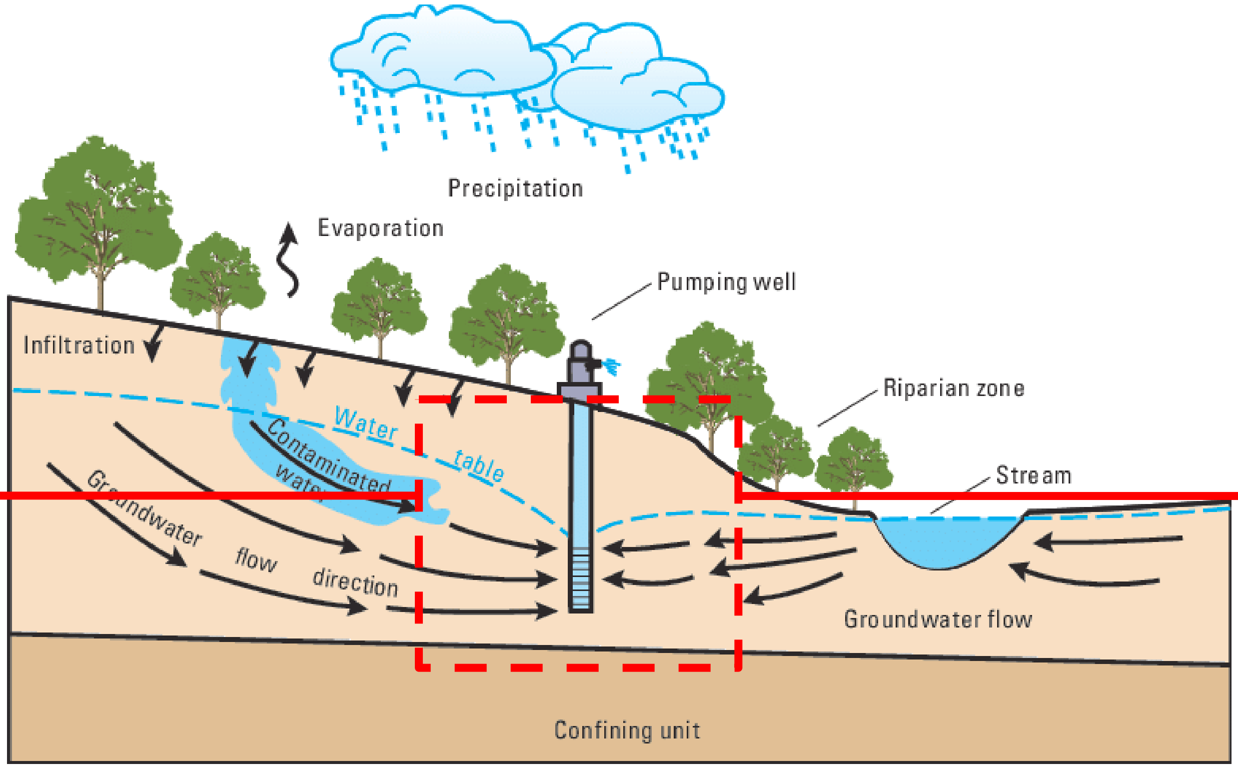

Hydraulic heads

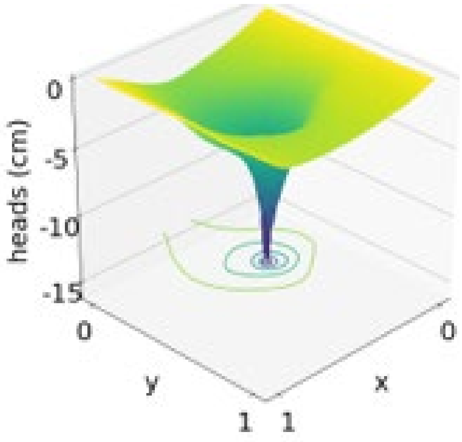

GW Forward and Inverse Problem

forward problem —parameterized PDEs→ Forward model is numerical method, e.g., finite element method (FEM) → Field dimension: n
Complexity: $O(n^2)$

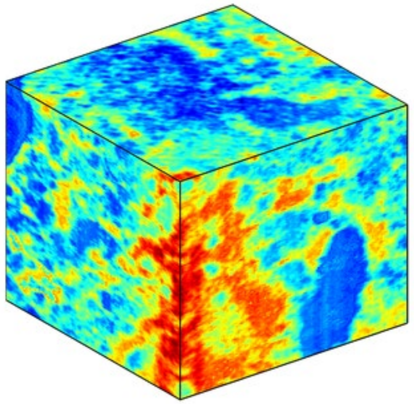

Forward

$T \in \mathbb{R}^{\mathrm{n}\times 1} \gg \mathbb{R}^{\mathrm{m}\times 1} \ni h$

Inverse

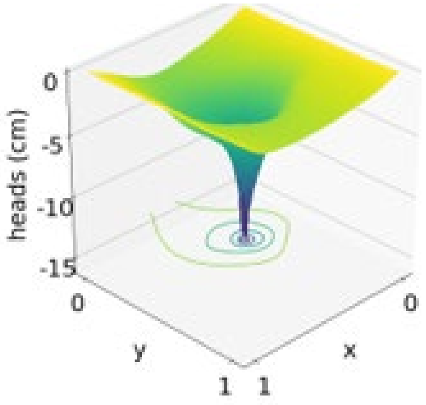

$$S_s \frac{\partial h}{\partial t} = -\nabla \cdot \mathbf{q} + Q \qquad \text{Mass conservation}$$

$$\mathbf{q} = T \nabla h \qquad \text{Darcy's Law}$$

S_s – specific storage; T – hydraulic transmissivity
h – hydraulic head; $\mathbf{q}$ – flux; Q – source/sink

inverse problem —non-linear and ill-posed→ Gradient-based inverse methods iteratively run forward model to determine Jacobian matrix, etc. → Computationally expensive & non-scalable

(Zhao & Luo, 2020; Zhao & Luo, 2021a; Zhao & Luo, 2021b; Zhao et al., 2022)

GW PINN Model

Groundwater PINNs (Tartakovsky et al., 2020)

$$NN(x^*, y^*) = h(x^*, y^*)$$
$$TNN(x^*, y^*) = T(x^*, y^*)$$

minimize →

$$||\mathcal{L}(T^*, h^*; x^*, y^*)||$$

Loss of PDE regularization

↑ governs

↑ soft constraint

Mass conservation

Darcy's Law

$$S_s \frac{\partial h}{\partial t} = -\nabla \cdot \mathbf{q} + Q$$
$$\mathbf{q} = T\nabla h$$

formulate →

$$\mathcal{L}(T^*, h^*; x^*, y^*) = 0$$

PDE residuals

$$\mathcal{L}(T^*, h^*; x^*, y^*) = \phi_n\left(T^*, h^*, \frac{\partial T^*}{\partial x^*}, \frac{\partial T^*}{\partial y^*}, \frac{\partial h^*}{\partial x^*}, \frac{\partial h^*}{\partial y^*}, \frac{\partial^2 T^*}{\partial x^{*2}}, \dots, \frac{\partial^n h^*}{\partial y^{*n}}\right)$$

Partial derivatives are evaluated with automatic differentiation

(He & Tartakovsky, 2021; Raissi et al., 2019; Tartakovsky et al., 2020; Wang et al., 2021; Xu et al., 2021)

Physical Constraints of Pumping Test

Aquifer (T): 2D, 1024×1024, confined & saturated, isotropic

$$S_s \frac{\partial h}{\partial t} = -\nabla \cdot \mathbf{q} + Q \qquad \text{Mass conservation}$$

$$\mathbf{q} = T\nabla h \qquad \text{Darcy's Law}$$

S_s – specific storage; T – hydraulic transmissivity

h – hydraulic head; $\mathbf{q}$ – flux; Q – source/sink

PDE for non-pumping grid	$S_s \frac{\partial h(x_e,y_e,t_e)}{\partial t} - \nabla \cdot [T(x_e,y_e)\nabla h(x_e,y_e,t_e)] = 0,$	$(x_e,y_e) \in \Omega, t_e \in (0,\mathrm{T}]$
PDE for pumping grid	$S_s \frac{\partial h(x_p,y_p,t_p)}{\partial t} - \nabla \cdot [T(x_p,y_p)\nabla h(x_p,y_p,t_p)] = Q_p,$	$(x_p,y_p) \in \Omega, t_p \in (0,\mathrm{T}]$
Neumann Boundary Condition	$\mathbf{n} \cdot \nabla h(x_N,y_N,t_N) = q_N,$	$(x_N,y_N) \in \Gamma_N, t_N \in (0,\mathrm{T}]$
Dirichlet Boundary Condition	$h(x_D,y_D,t_D) = h_D,$	$(x_D,y_D) \in \Gamma_D, t_D \in (0,\mathrm{T}]$
Initial Condition	$h(x_{init},y_{init},0) = h_{init},$	$(x_{init},y_{init}) \in \Omega$

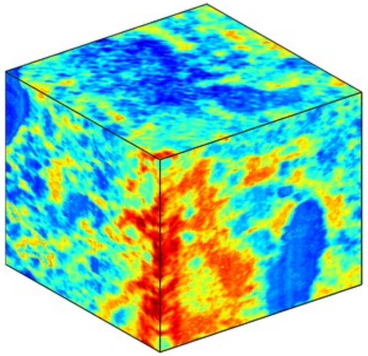

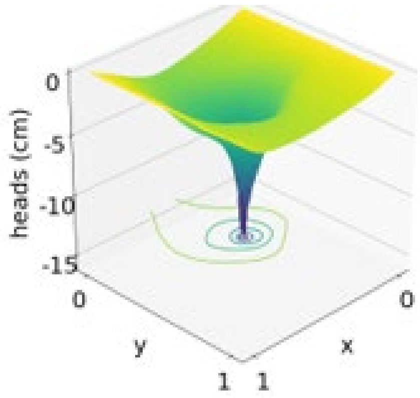

PLAN View

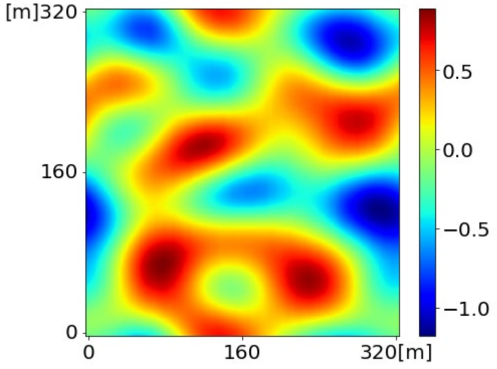

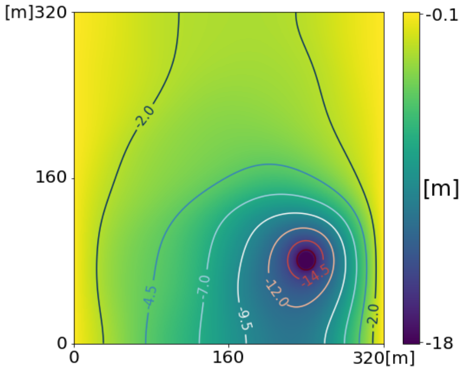

(Guo et al., 2022)

Network Structure

DNN model:

$$h(x,y,t) \approx NN(x,y,t)$$
$$T(x,y) \approx TNN(x,y)$$

Data (reference):

Monitored hydraulic heads: $NN(x_m, y_m) = h_m$

Measurements of transmissivity: $TNN(x_T, y_T) = T(x_T, y_T)$

Regularization (collocation):

$$S_s \frac{\partial NN(x_e,y_e,t_e)}{\partial t} - \nabla \cdot [TNN(x_e,y_e)\nabla NN(x_e,y_e,t_e)] = 0$$

$$S_s \frac{\partial NN(x_p,y_p,t_p)}{\partial t} - \nabla \cdot [TNN(x_p,y_p)\nabla NN(x_p,y_p,t_p)] = Q_p$$

$$\mathbf{n} \cdot \nabla NN(x_N,y_N,t_N) = q_N$$

$$NN(x_D,y_D,t_D) = h_D$$

$$NN(x_{init},y_{init},0) = h_{init}$$

Forward Net   Inverse Net

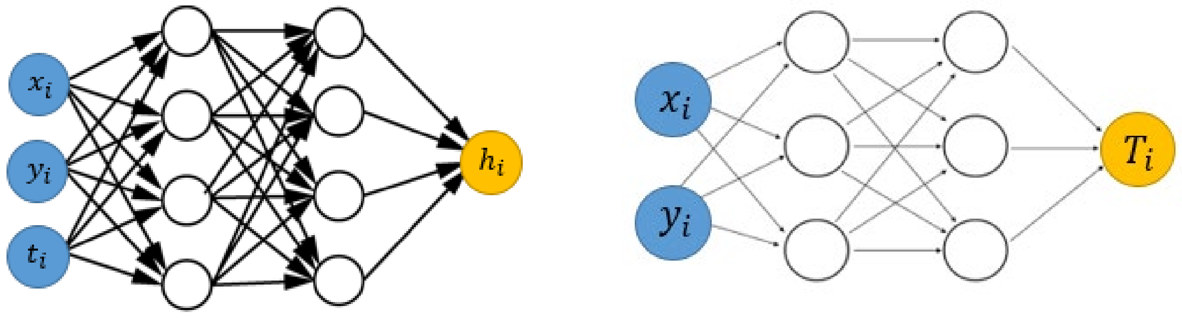

Network Architecture

	Transient Forward	Inverse
Input variables	Spatial & temporal (x,y,t)	Spatial (x,y)
Output variables	Hydraulic heads (h)	Transmissivity (T)
Number of layers	7	
Hidden dimensions	50	
Activation function	Hyperbolic $(tanh)$	
Output layer type	Linear	

(Guo et al., 2022)

Data Batch Sampling

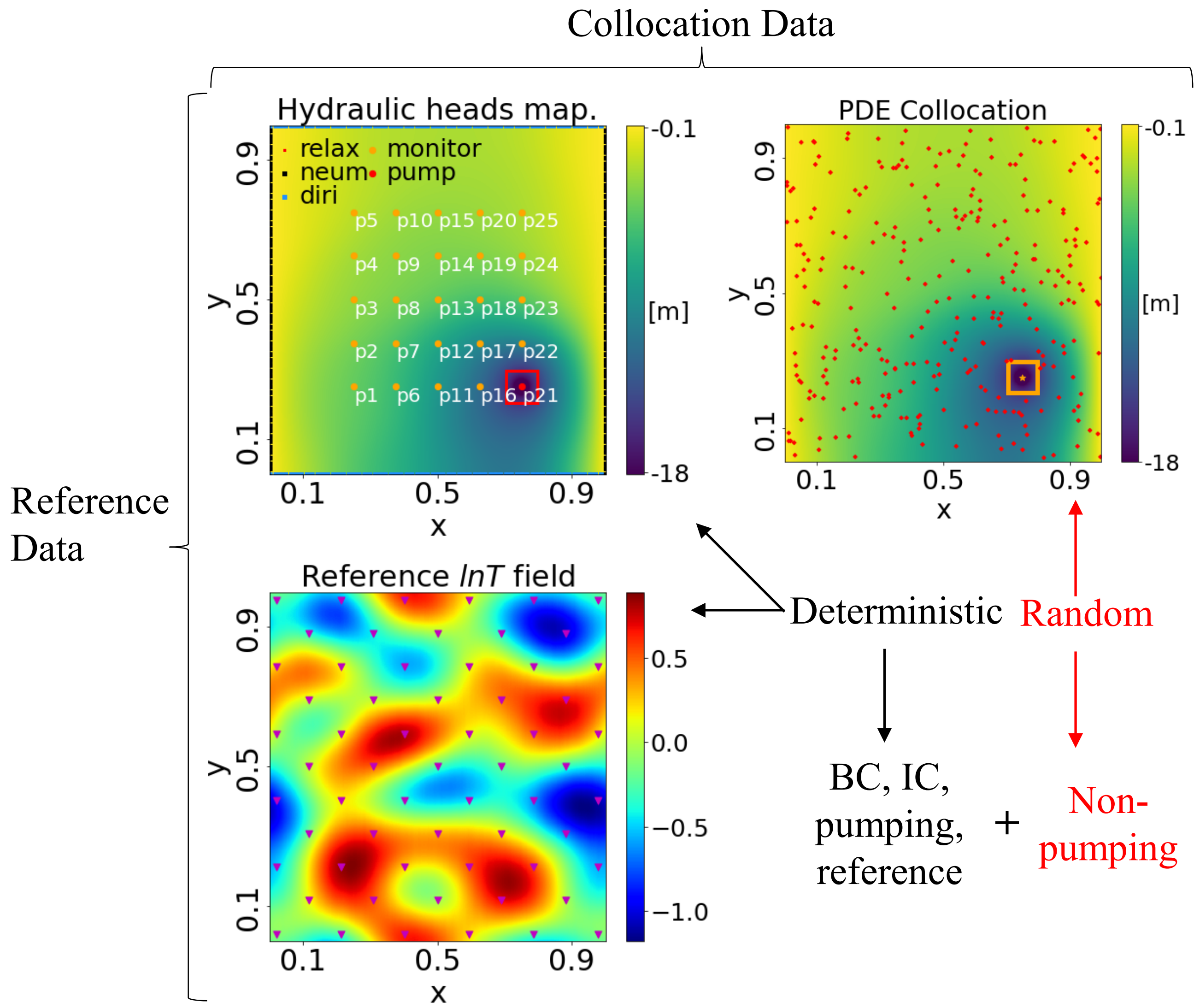

= **Data Batch**

Composition of training data in each batch for HT-PINN

Type of points	**Pumping**	**Time**	**Batch**	**Number**
Pumping (x_p, y_p)	Invariant	Invariant	Invariant	1
Neumann (x_N, y_N)	Invariant	Invariant	Invariant	64 × 2
Dirichlet (x_D, y_D)	Invariant	Invariant	Invariant	64 × 2
Direct (x_T, y_T)	Invariant	Invariant	Invariant	61
Initial (x_{init}, y_{init})	Variant	Invariant	Invariant	25
Monitored (x_m, y_m, t_m)	Variant	Variant	Invariant	24
Non-pumping (x_e, y_e, t_e)	Variant	Variant	Variant	300

SCIENCE LEADS THE FUTURE

(Guo et al., 2022)

PINN for Transient Pumping Test

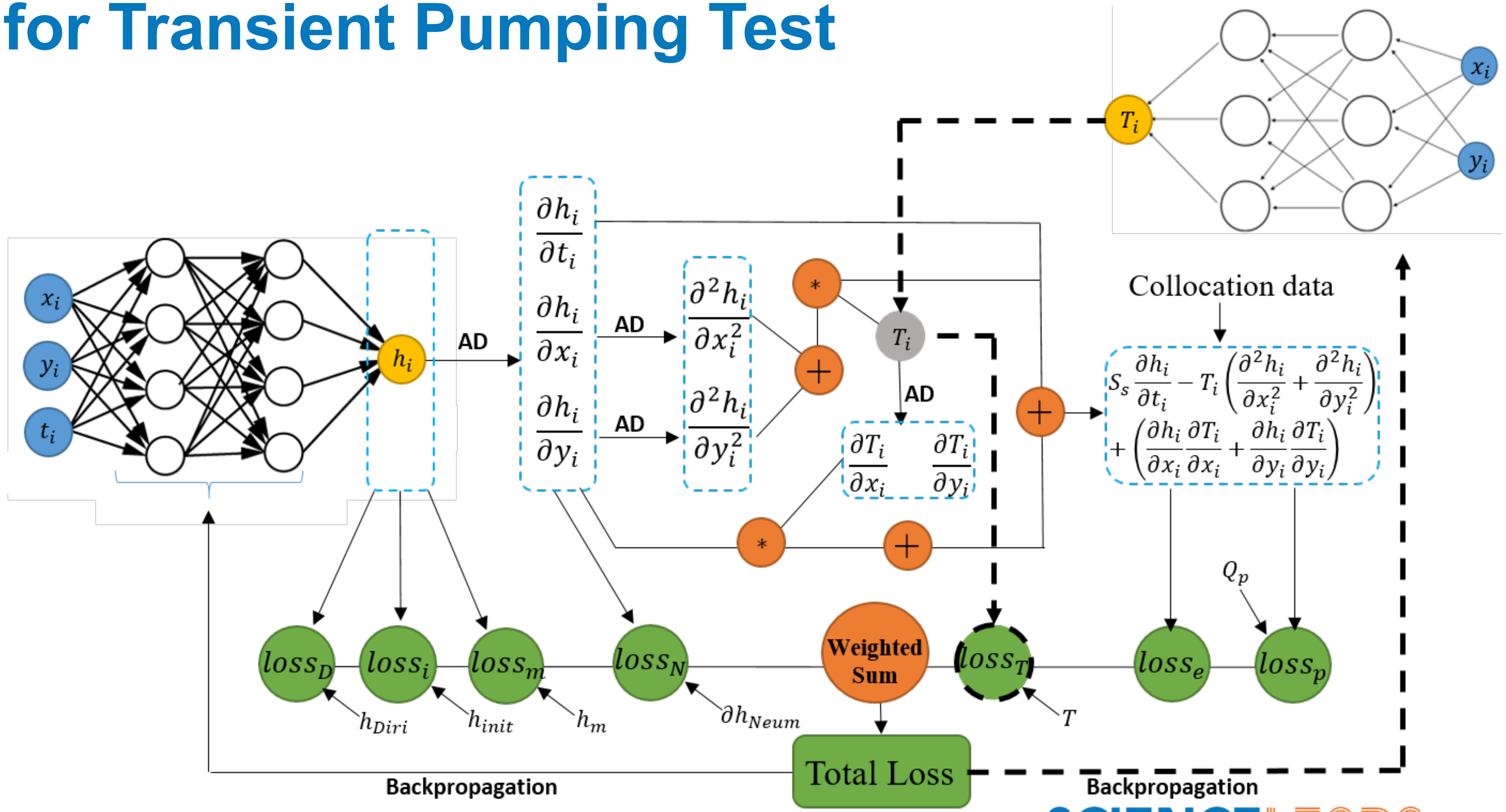

(Guo et al., 2022)

Hydraulic Tomography - PINN

One inverse network TNN

Total loss of HT-PINN:

$$\ell_{\mathrm{HT-PINN}} = \sum \ell_{NN^i} + \ell_{TNN}$$

Each pumping test has a forward network NN^i

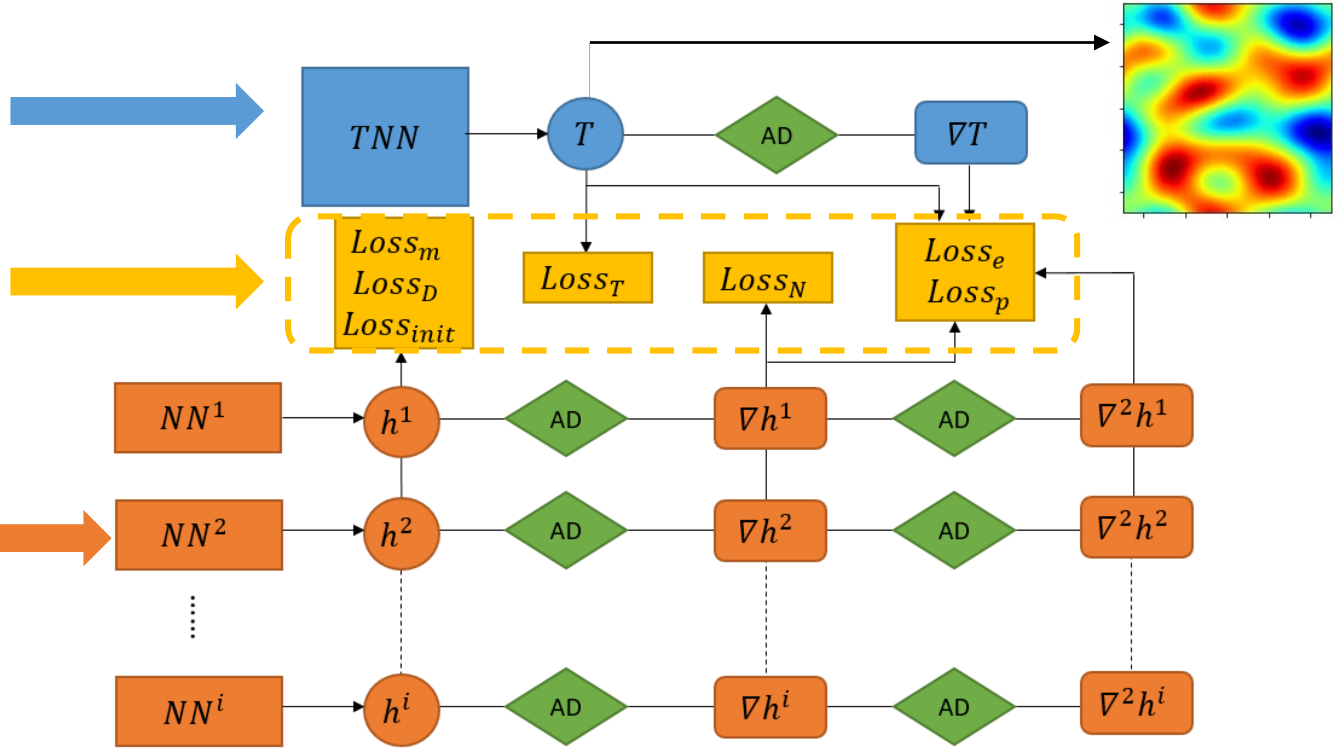

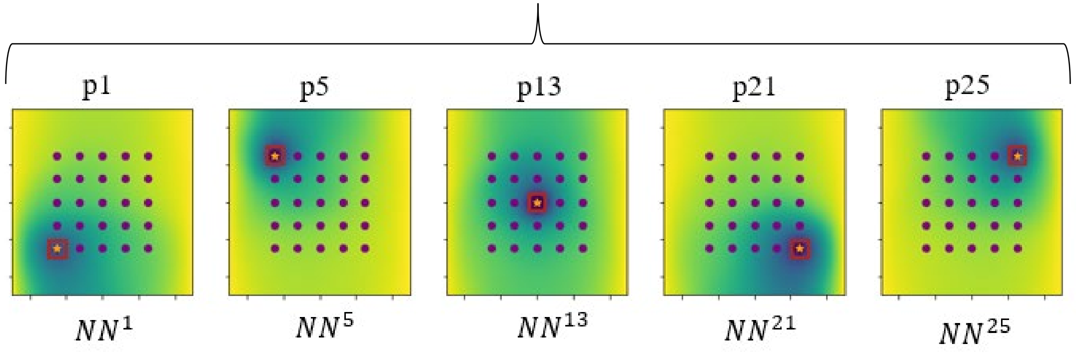

(Guo et al., 2022)

AGU FALL MEETING

Transient Forward Prediction

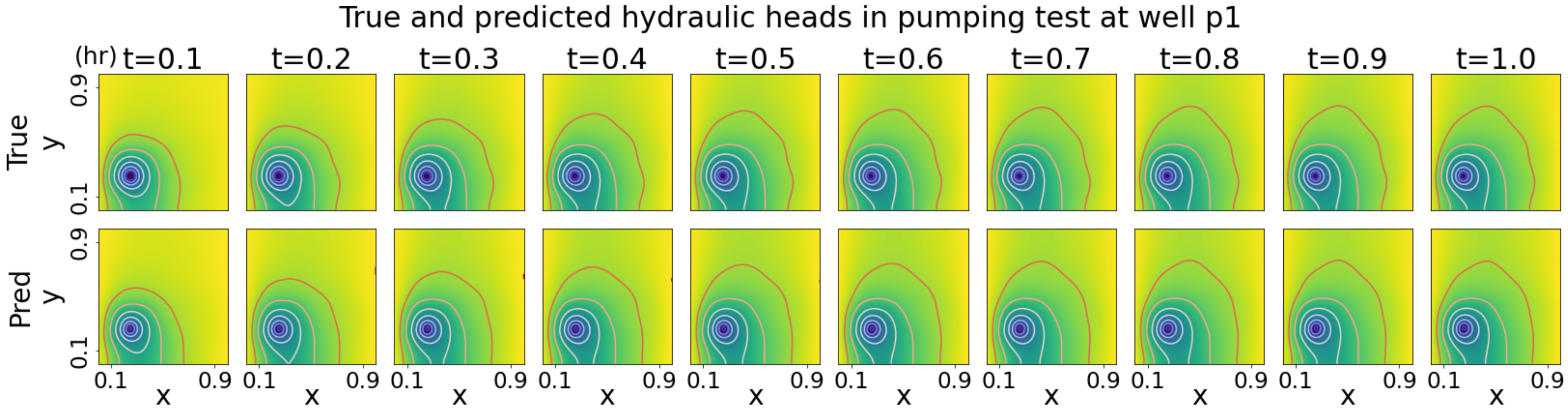

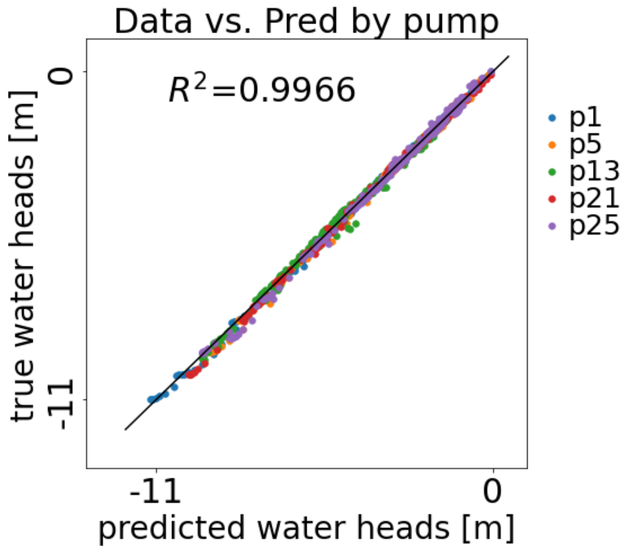

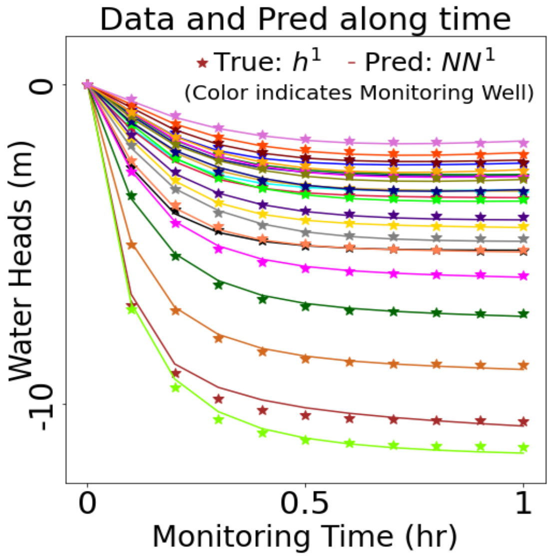

Average relative residual $\epsilon_{NN_t^i}$ average on all time steps $t = 0.1 - 1.0$:

- P1: 6.14%
- P5: 6.26%
- P13: 6.23%
- P21: 6.58%
- P25: 6.53%

SCIENCE LEADS THE FUTURE

(Guo et al., 2022)

Inverse Estimation

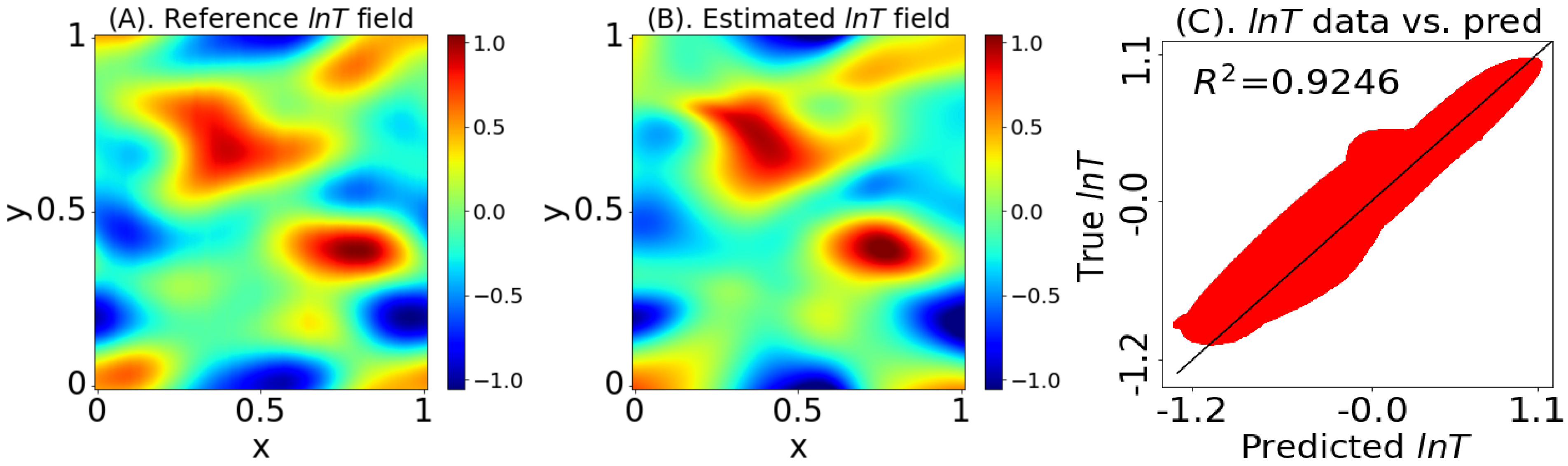

The relative residual ϵ_{TNN} is 10.32%, and the accuracy is 94.93%.

Training time is about 9.5 hours.

(Guo et al., 2022)

Model Scalability

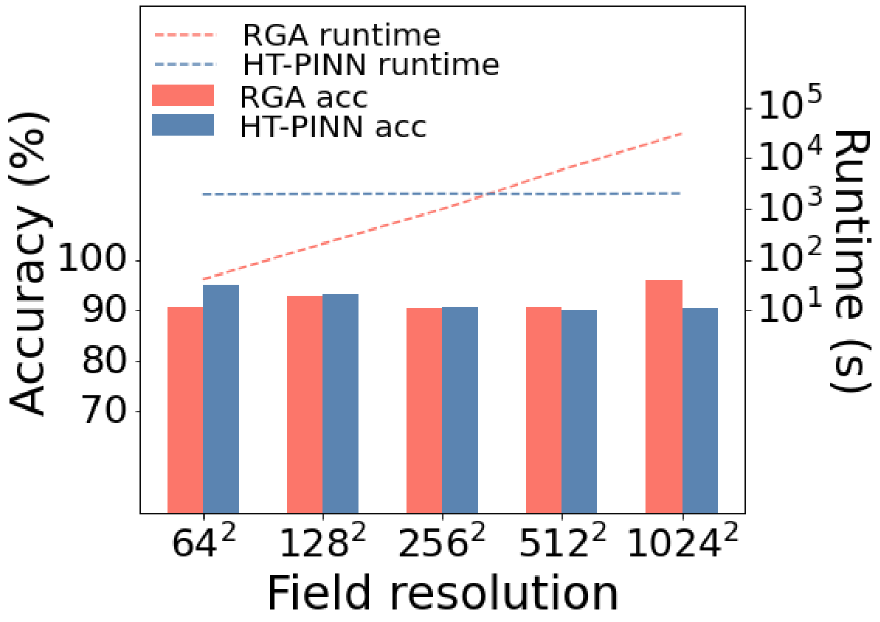

Model	RGA	HT-PINN
Accuracy	> 90%	> 90%
N_h	24×5	24×5
N_{lnT}	0	61
Covariance	Yes	No
Scalability	Linear	Constant

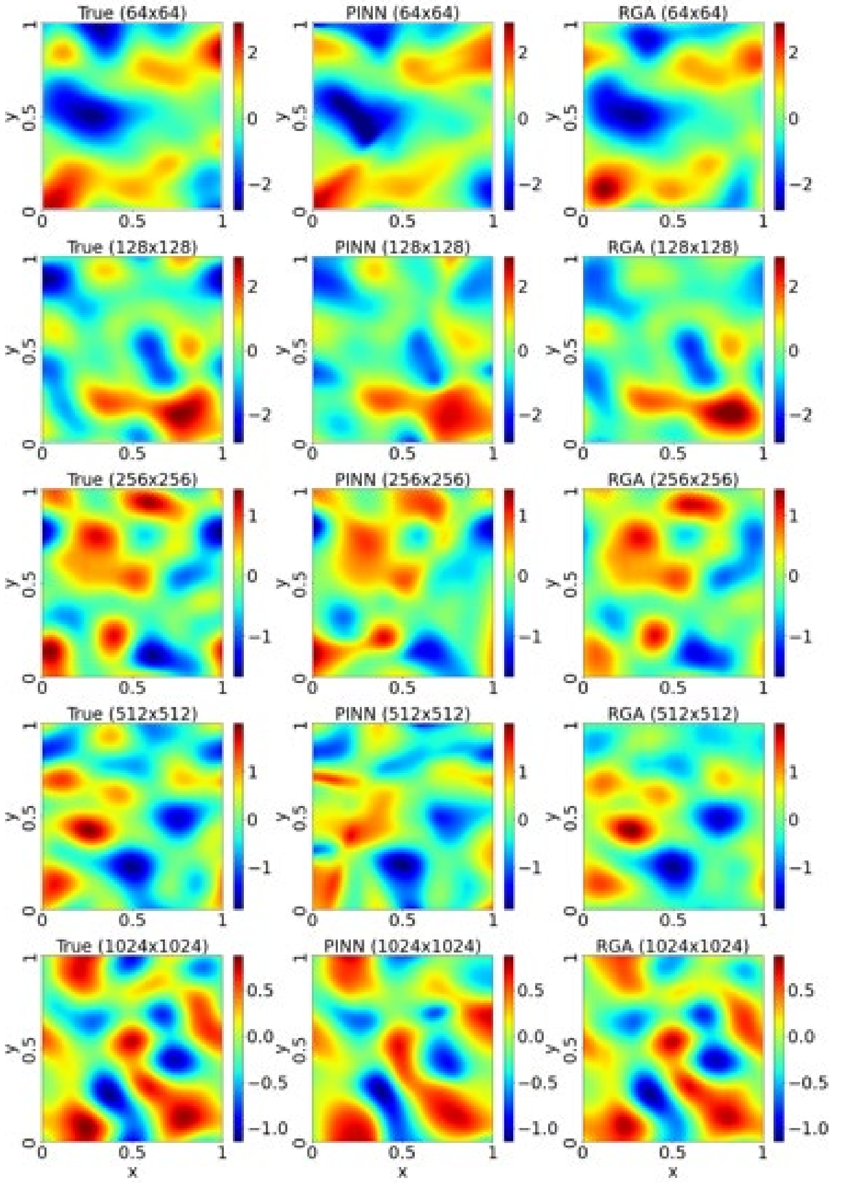

Future improvements:

- Data efficiency: reduce amount of reference data
- Generalizability: applicable to non-Gaussian field

(Guo et al., 2022)

Many thanks for your time!

Appreciate any questions

Acknowledgements: thanks many peers for sharing their work of applying machine learning to subsurface modeling where we get inspirations and guidance from, especially Dr. A.M, Tartakovsky, Dr. D, Zhang, Dr. N, Wang, Dr. Q, He, Dr. E, Laloy, Dr. R, Xu, etc.

Reference

Bandai, T., & Ghezzehei, T. A. (2021), Physics-Informed Neural Networks With Monotonicity Constraints for Richardson-Richards Equation: Estimation of Constitutive Relationships and Soil Water Flux Density From Volumetric Water Content Measurements, *Water Resources Research*, *57*(2), e2020WR027642.
Bottou, L., & Bousquet, O. (2008), The tradeoffs of large scale learning, *Adv. Neur. In*, *20*, 161-168.
Broyden, C. G. (1965), A class of methods for solving nonlinear simultaneous equations, *Math. Comput.*, *19*(92), 577-593.
Cardiff, M., Barrash, W., & Kitanidis, P. K. (2013), Hydraulic conductivity imaging from 3-D transient hydraulic tomography at several pumping/observation densities, *Water Resour. Res.*, *49*(11), 7311-7326.
Carrera, J., & Neuman, S. P. (1986), Estimation of Aquifer Parameters Under Transient and Steady State Conditions: 1. Maximum Likelihood Method Incorporating Prior Information, *Water Resources Research*, *22*(2), 199-210.
Cheng, S., Cheng, L., Qin, S., Zhang, L., Liu, P., Liu, L., Xu, Z., & Wang, Q. (2022), Improved Understanding of How Catchment Properties Control Hydrological Partitioning Through Machine Learning, *Water Resources Research*, *58*(4), e2021WR031412.
Cho, E., Jacobs, J. M., Jia, X., & Kraatz, S. (2019), Identifying Subsurface Drainage using Satellite Big Data and Machine Learning via Google Earth Engine, *Water Resources Research*, *55*(10), 8028-8045.
Fienen, M. N., Clemo, T., & Kitanidis, P. K. (2008), An interactive Bayesian geostatistical inverse protocol for hydraulic tomography, *Water Resources Research*, *44*(12).
Goldberg, Y. (2016), A primer on neural network models for natural language processing, *J. Artif. Int. Res.*, *57*(1), 345–420.
Goldstein, E. B., & Coco, G. (2014), A machine learning approach for the prediction of settling velocity, *Water Resources Research*, *50*(4), 3595-3601.
Griewank, A. (2003), A mathematical view of automatic differentiation, *Acta Numer.*, *12*, 321-398.
Guo, Q., Zhao, Y., Lu, C., Luo, J., 2022. High-dimensional inverse modeling of hydraulic tomography by physics informed neural network (HT-PINN). J. Hydrol., 128828. DOI:https://doi.org/10.1016/j.jhydrol.2022.128828
He, Q., & Tartakovsky, A. M. (2021), Physics-Informed Neural Network Method for Forward and Backward Advection-Dispersion Equations, *Water Resources Research*, *57*(7), e2020WR029479.
He, Q., Barajas-Solano, D., Tartakovsky, G., & Tartakovsky, A. M. (2020a), Physics-informed neural networks for multiphysics data assimilation with application to subsurface transport, *Advances in Water Resources*, *141*, 103610.
He, Q., Barajas-Solano, D., Tartakovsky, G., & Tartakovsky, A. M. (2020b), Physics-informed neural networks for multiphysics data assimilation with application to subsurface transport, *Adv. Water Resour.*, *141*, 103610.
Hoffer, E., Hubara, I., & Soudry, D. (2018), Train longer, generalize better: closing the generalization gap in large batch training of neural networks, *arXiv*.
Hofmann, T. (2004), Latent semantic models for collaborative filtering, *ACM Trans. Inf. Syst.*, *22*(1), 89-115.
Ioffe, S., & Szegedy, C. (2015), Batch Normalization: Accelerating Deep Network Training by Reducing Internal Covariate Shift, in *Proceedings of the 32nd International Conference on Machine Learning*, edited by B. Francis and B. David, pp. 448--456, PMLR, Proceedings of Machine Learning Research.
Jacob, Dillavou, S., Stern, M., Andrea, & Douglas (2022), Learning Without a Global Clock: Asynchronous Learning in a Physics-Driven Learning Network, *arXiv*.

(Guo et al., 2022)

Reference

Jagtap, A. D., Kharazmi, E., & Karniadakis, G. E. (2020), Conservative physics-informed neural networks on discrete domains for conservation laws: Applications to forward and inverse problems, *Comput. Methods Appl. Mech. Eng.*, *365*, 113028.

Kang, P. K., Lee, J., Fu, X., Lee, S., Kitanidis, P. K., & Juanes, R. (2017), Improved characterization of heterogeneous permeability in saline aquifers from transient pressure data during freshwater injection, *Water Resour. Res.*, *53*(5), 4444-4458.

Karniadakis, G. (2019), VPINNs: Variational physics-informed neural networks for solving partial differential equations, *arXiv*.

Kharazmi, E., Zhang, Z., & Karniadakis, G. E. M. (2021), hp-VPINNs: Variational physics-informed neural networks with domain decomposition, *Comput. Methods Appl. Mech. Eng.*, *374*, 113547.

Kingma, D. P., & Ba, J. (2017), Adam: A Method for Stochastic Optimization, *arXiv*.

Kitanidis, P. K. (1995), Quasi-Linear Geostatistical Theory for Inversing, *Water Resour. Res.*, *31*(10), 2411-2419.

Kitanidis, P. K., & Vomvoris, E. G. (1983), A geostatistical approach to the inverse problem in groundwater modeling (steady state) and one-dimensional simulations, *Water Resources Research*, *19*(3), 677-690.

Klein, O., Cirpka, O. A., Bastian, P., & Ippisch, O. (2017), Efficient geostatistical inversion of transient groundwater flow using preconditioned nonlinear conjugate gradients, *Adv. Water Resour.*, *102*, 161-177.

Krizhevsky, A., Sutskever, I., & Hinton, G. E. (2012), ImageNet classification with deep convolutional neural networks, paper presented at Adv. Neur. In.

Laloy, E., Hérault, R., Lee, J., Jacques, D., & Linde, N. (2017), Inversion using a new low-dimensional representation of complex binary geological media based on a deep neural network, *Advances in water resources*, *110*, 387-405.

LeCun, Y., Bengio, Y., & Hinton, G. (2015), Deep learning, *Nature*, *521*(7553), 436-444.

Lee, J., & Kitanidis, P. (2014), Large scale hydraulic tomography and joint inversion of head and tracer data using the Principal Component Geostatistical Approach (PCGA), *Water Resour. Res.*, *50*, 5410-5427.

Li, J., & Tartakovsky, A. M. (2022), Physics-informed Karhunen-Loéve and neural network approximations for solving inverse differential equation problems, *J. Comput. Phys.*, *462*, 111230.

Li, J., Wang, Z., Wu, X., Xu, C.-Y., Guo, S., Chen, X., & Zhang, Z. (2021), Robust Meteorological Drought Prediction Using Antecedent SST Fluctuations and Machine Learning, *Water Resources Research*, *57*(8), e2020WR029413.

Li, M., Zhang, T., Chen, Y., & Smola, A. J. (2021), Efficient mini-batch training for stochastic optimization, ACM, 2014.

Liu, X., & Kitanidis, P. (2011), Large-scale inverse modeling with an application in hydraulic tomography, *Water Resour. Res.*, *47*(2).

Liu, Y., Sun, W., & Durlofsky, L. (2019), A Deep-Learning-Based Geological Parameterization for History Matching Complex Models, *Mathematical Geosciences*, *51*.

Masters, D., & Luschi, C. (2018), Revisiting Small Batch Training for Deep Neural Networks, *arXiv*.

McCandlish, S., Kaplan, J., Amodei, D., & OpenAi (2018), An Empirical Model of Large-Batch Training, *arXiv*.

Meyer, D., Grimmond, S., Dueben, P., Hogan, R., & van Reeuwijk, M. (2022), Machine Learning Emulation of Urban Land Surface Processes, *Journal of Advances in Modeling Earth Systems*, *14*(3), e2021MS002744.

Neuman, S. P. (1980), A statistical approach to the inverse problem of aquifer hydrology: 3. Improved solution method and added perspective, *Water Resources Research*, *16*(2), 331-346.

(Guo et al., 2022)

Reference

Nitish, Mudigere, D., Nocedal, J., Smelyanskiy, M., & Ping (2017), On Large-Batch Training for Deep Learning: Generalization Gap and Sharp Minima, *arXiv*.
Nowak, W., Tenkleve, S., & Cirpka, O. A. (2003), Efficient computation of linearized cross-covariance and auto-covariance matrices of interdependent quantities, *Math. Geol.*, *35*(1), 53-66.
Pang, G., D'Elia, M., Parks, M., & Karniadakis, G. (2020), nPINNs: Nonlocal physics-informed neural networks for a parametrized nonlocal universal Laplacian operator. Algorithms and applications, *J. Comput. Phys.*, *422*, 109760.
Rahmati, O., Naghibi, S. A., Shahabi, H., Bui, D. T., Pradhan, B., Azareh, A., Rafiei-Sardooi, E., Samani, A. N., & Melesse, A. M. (2018), Groundwater spring potential modelling: Comprising the capability and robustness of three different modeling approaches, *Journal of Hydrology*, *565*, 248-261.
Raissi, M., Perdikaris, P., & Karniadakis, G. (2017a), Physics Informed Deep Learning (Part II): Data-driven Discovery of Nonlinear Partial Differential Equations, *arXiv*, *abs/1711.10566*.
Raissi, M., Perdikaris, P., & Karniadakis, G. (2017b), Physics Informed Deep Learning (Part I): Data-driven Solutions of Nonlinear Partial Differential Equations, *arXiv*, *abs/1711.10561*.
Raissi, M., Perdikaris, P., & Karniadakis, G. E. (2019), Physics-informed neural networks: A deep learning framework for solving forward and inverse problems involving nonlinear partial differential equations, *J. Comput. Phys.*, *378*, 686-707.
Ren, P., Rao, C., Liu, Y., Wang, J.-X., & Sun, H. (2021), *PhyCRNet: Physics-informed Convolutional-Recurrent Network for Solving Spatiotemporal PDEs*.
Saibaba, A. K., Ambikasaran, S., Li, J. Y., Kitanidis, P. K., & Darve, E. F. (2012), Application of hierarchical matrices to linear inverse problems in geostatistics, *Oil. Gas. Sci. Technol*, *67*(5), 857-875.
Shahnas, M. H., Yuen, D. A., & Pysklywec, R. N. (2018), Inverse Problems in Geodynamics Using Machine Learning Algorithms, *J. Geophys. Res.: Solid Earth*, *123*(1), 296-310.
Snodgrass, M. F., & Kitanidis, P. K. (1998), Transmissivity identification through multi-directional aquifer stimulation, *Stochastic Hydrology and Hydraulics*, *12*(5), 299-316.
Sun, A. Y., Scanlon, B. R., Save, H., & Rateb, A. (2021), Reconstruction of GRACE Total Water Storage Through Automated Machine Learning, *Water Resources Research*, *57*(2), e2020WR028666.
Tahmasebi, P. (2017), HYPPS: A hybrid geostatistical modeling algorithm for subsurface modeling, *Water Resources Research*, *53*(7), 5980-5997.
Tartakovsky, A. M., Marrero, C. O., Perdikaris, P., Tartakovsky, G. D., & Barajas-Solano, D. (2020), Physics-Informed Deep Neural Networks for Learning Parameters and Constitutive Relationships in Subsurface Flow Problems, *Water Resour. Res., 56*(5), e2019WR026731, doi: https://doi.org/10.1029/2019WR026731.
Vo, H. X., & Durlofsky, L. J. (2014), A New Differentiable Parameterization Based on Principal Component Analysis for the Low-Dimensional Representation of Complex Geological Models, *Mathematical Geosciences*, *46*(7), 775-813.
Wang, N., Chang, H., & Zhang, D. (2021a), Deep-Learning-Based Inverse Modeling Approaches: A Subsurface Flow Example, *J. Geophys. Res.: Solid Earth*, *126*(2), e2020JB020549.
Wang, N., Chang, H., & Zhang, D. (2021b), Efficient uncertainty quantification for dynamic subsurface flow with surrogate by Theory-guided Neural Network, *Comput. Methods Appl. Mech. Eng.*, *373*, 113492.
Wang, N., Zhang, D., Chang, H., & Li, H. (2020), Deep learning of subsurface flow via theory-guided neural network, *J. Hydrol.*, *584*, 124700.
Wilson, D. R., & Martinez, T. R. (2003), The general inefficiency of batch training for gradient descent learning, *Neural Networks*, *16*(10), 1429-1451.

(Guo et al., 2022)

Reference

Xu, R., Wang, N., & Zhang, D. (2021a), Solution of diffusivity equations with local sources/sinks and surrogate modeling using weak form Theory-guided Neural Network, *Adv. Water Resour.*, *153*, 103941.
Xu, R., Zhang, D., Rong, M., & Wang, N. (2021b), Weak form theory-guided neural network (TgNN-wf) for deep learning of subsurface single- and two-phase flow, *J. Comput. Phys.*, *436*, 110318.
Yan, J., Jia, S., Lv, A., & Zhu, W. (2019), Water Resources Assessment of China's Transboundary River Basins Using a Machine Learning Approach, *Water Resources Research*, *55*(1), 632-655.
Yang, L., Zhang, D., & Karniadakis, G. E. (2020), Physics-Informed Generative Adversarial Networks for Stochastic Differential Equations, *SIAM J. Sci. Comput.*, *42*(1), A292-A317.
Yang, L., Meng, X., & Karniadakis, G. E. (2021), B-PINNs: Bayesian physics-informed neural networks for forward and inverse PDE problems with noisy data, *J. Comput. Phys.*, *425*, 109913.
Yang, Y., & Perdikaris, P. (2019), Adversarial Uncertainty Quantification in Physics-Informed Neural Networks, *J. Comput. Phys.*, *394*, 136-152.
Yeh, T., & Liu, S. (2000), Hydraulic tomography: Development of a new aquifer test method, *Water Resour. Res.*, *36*, 2095-2105.
Yeh, T., Jin, M., & Hanna, S. (1995), An Iterative Stochastic Inverse Method: Conditional Effective Transmissivity and Hydraulic Head Fields.
Yeh, T. C., & Lee, C. H. (2007), Time to change the way we collect and analyze data for aquifer characterization, *Ground water*, *45*(2), 116-118.
Zhao, W. L., Gentine, P., Reichstein, M., Zhang, Y., Zhou, S., Wen, Y., Lin, C., Li, X., & Qiu, G. Y. (2019), Physics-Constrained Machine Learning of Evapotranspiration, *Geophysical Research Letters*, *46*(24), 14496-14507.
Zhao, Y., & Luo, J. (2020), Reformulation of Bayesian Geostatistical Approach on Principal Components, *Water Resour. Res.*, *56*.
Zhao, Y., & Luo, J. (2021a), Bayesian inverse modeling of large-scale spatial fields on iteratively corrected principal components, *Adv. Water Resour.*, *151*, 103913.
Zhao, Y., & Luo, J. (2021b), A Quasi-Newton Reformulated Geostatistical Approach on Reduced Dimensions for Large-Dimensional Inverse Problems, *Water Resour. Res.*, *57*(1), e2020WR028399.
Zhu, Y., Zabaras, N., Koutsourelakis, P.-S., & Perdikaris, P. (2019), Physics-constrained deep learning for high-dimensional surrogate modeling and uncertainty quantification without labeled data, *J. Comput. Phys.*, *394*, 56-81.

(Guo et al., 2022)

Appendix – Experimental Domain

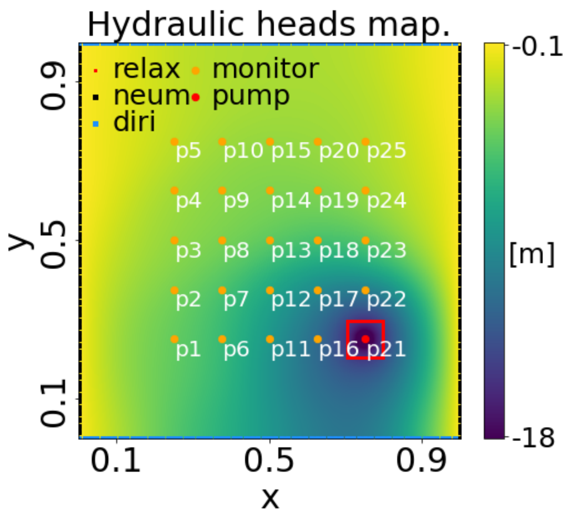

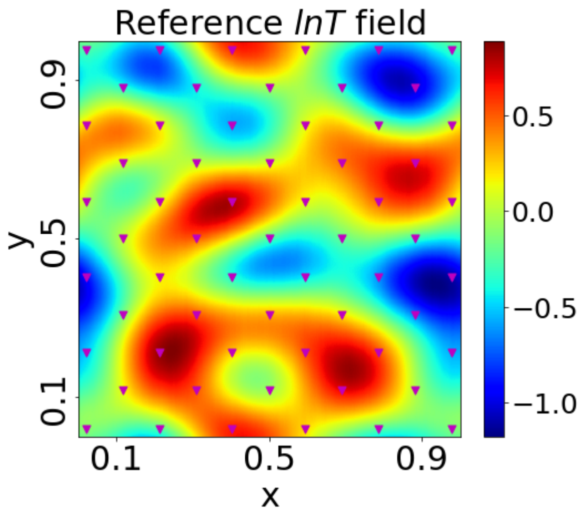

Hydrogeological and geostatistical parameters for the hydraulic tomography experiment

Parameter	Values
Domain size, $L_x \times L_y$	320m × 320m
Grid spacing, $\Delta x \times \Delta y$	0.3125m × 0.3125m
Spatial resolution, $n_x \times n_y$	1024 × 1024
Transmissivity, T [m^2/hr]	
Geometric mean	0
Variance of ln$T$, σ^2_{lnT}	1
Correlation length, $\lambda_x \times \lambda_y$	64m × 48m
Left Boundary	h=0m
Right Boundary	h=0m
Initial Condition	h=0m
Pumping Time [hr]	1
Monitor Time Step [hr]	0.1
Pumping Rate [m^3/hr]	3.6

Appendix – PDE Loss

Physical Constraints:

$$S_s \frac{\partial h(x_e,y_e,t_e)}{\partial t} - \nabla \cdot [T(x_e,y_e)\nabla h(x_e,y_e,t_e)] = 0,$$

PDE residual:

$$f_{NN^i,TNN}(x,y,t) = S_s \frac{\partial NN^i(x,y,t)}{\partial t} - \nabla \cdot [TNN(x,y)\nabla NN^i(x,y,t)],$$

PDE for non-pumping grid:

$$Loss_e = \frac{1}{N_e}\sum_{j=1}^{N_e} \left| f_{NN,TNN}\left(x_e^j, y_e^j, t_e^j\right)\right|^2$$

PDE for pumping grid:

$$Loss_p = \frac{1}{N_p}\sum_{j=1}^{N_p} \left| f_{NN,TNN}\left(x_p^j, y_p^j, t_p^j\right) - Q_p\right|^2$$

Appendix – B.C and I.C Loss

Dirichlet B.C.:

$$Loss_D = \frac{1}{N_D}\sum_{j=1}^{N_D}\left|NN\left(x_D^j, y_D^j, t_D^j\right) - h\left(x_D^j, y_D^j, t_D^j\right)\right|^2$$

Neumann B.C.:

$$Loss_N = \frac{1}{N_N}\sum_{j=1}^{N_N}\left|\boldsymbol{n} \cdot \nabla NN\left(x_N, y_N, t_N\right) - q_N\right|^2$$

Initial Condition:

$$Loss_{init} = \frac{1}{N_{init}}\sum_{j=1}^{N_{init}}|NN(x_{init}, y_{init}, 0) - h(x_{init}, y_{init}, 0)|^2$$

Appendix – Data Match Loss

Monitored Hydraulic Heads:

$$Loss_m = \frac{1}{N_m} \sum_{j=1}^{N_m} \left| NN\left(x_m^j, y_m^j, t_m^j\right) - h\left(x_m^j, y_m^j, t_m^j\right) \right|^2$$

Measured Transmissivity:

$$Loss_T = \frac{1}{N_T} \sum_{j=1}^{N_T} \left| TNN\left(x_T^j, y_T^j\right) - T\left(x_T^j, y_T^j\right) \right|^2$$

Appendix – Loss Function

$$Loss_{NN} = \lambda_m Loss_m + \lambda_e Loss_e + \lambda_N Loss_N + \lambda_D Loss_D + \lambda_p Loss_p + \lambda_{init} Loss_{init}$$

$$Loss_{HT-PINN} = \sum_{i=1,2,\ldots n} Loss_{NN}^{i} + \lambda_T Loss_T$$

$$\lambda_m = 10^4, \lambda_f = 50, \lambda_p = 1, \lambda_N = 10^4, \lambda_D = 2 \times 10^4, \lambda_T = 10^3, \lambda_{init} = 10^4$$

Appendix – Evaluation Met

Relative residuals:

$$\epsilon_{NN^i} = \frac{\left\|\boldsymbol{NN^i}(x,y,t) - \boldsymbol{h^i}(x,y,t)\right\|_2^2}{\|\boldsymbol{h^i}(x,y,t)\|_2^2}, (x,y) \in \Omega, t \in (0, \mathrm{T}]$$

$$\epsilon_T = \frac{\|\boldsymbol{TNN}(x,y) - \boldsymbol{T}(x,y)\|_2^2}{\|\boldsymbol{T}(x,y)\|_2^2}, (x,y) \in \Omega$$

Inverse accuracy:

$$\varepsilon(x,y) = \frac{|TNN(x,y) - T(x,y)|}{T^{max} - T^{min}}, (x,y) \in \Omega$$

Accuracy = percent of grids with $\varepsilon(x,y) < 10\%$

Appendix – Training Implementation

- 5 forward networks + 1 inverse network are trained together.
- Reference data are corrupted with 5% white noises.
- Input and output variables are normalized.
- Different loss terms are weighted to similar magnitude.
- Each training iteration takes a batch of data to feed HT-PINN.
- Each epoch has 50 iterations for steady-state and 500 iterations for transient HT.
- HT-PINN is trained for 3000 epochs with Adam optimizer.
- Learning rate = 10^{-3} for 1-1000, 10^{-4} for 1000-2000, 10^{-5} for 2000-3000.
- Training hardwares are Google Colab GPU